BOREAL ENVIRONMENT RESEARCH 14: 641–653
ISSN 1239-6095 (print) ISSN 1797-2469 (online)

Helsinki 31 August 2009

Observations of aerosol–cloud interactions at the Puijo semi-urban measurement station

Harri J. Portin[1)], Mika Komppula[1)], Ari P. Leskinen[1)], Sami Romakkaniemi[2)], Ari Laaksonen[2)3)] and Kari E. J. Lehtinen[1)2)]

[1)] *Finnish Meteorological Institute, Kuopio Unit, P.O. Box 1627, FI-70211 Kuopio, Finland*
[2)] *University of Kuopio, Department of Physics, P.O. Box 1627, FI-70211 Kuopio, Finland*
[3)] *Finnish Meteorological Institute, Research and Development, P.O. Box 503, FI-00101 Helsinki, Finland*

Received 16 Dec. 2008, accepted 25 Feb. 2009 (Editor in charge of this article: Veli-Matti Kerminen)

Portin, H. J., Komppula, M., Leskinen, A. P., Romakkaniemi, S., Laaksonen, A. & Lehtinen, K. E. J. 2009: Observations of aerosol–cloud interactions at the Puijo semi-urban measurement station. *Boreal Env. Res.* 14: 641–653.

The Puijo measurement station has produced continuous data on aerosol–cloud interactions since June 2006. The station is located on the top floor of an observation tower in a semi-urban environment near the town of Kuopio in central Finland. The top of the tower (306 m a.s.l.) has been detected to be in-cloud approximately 10% of the time. We analysed continuous weather, particle size distribution and cloud droplet size distribution measurements. The effects of local pollutant sources and air mass origin on aerosol–cloud interaction were examined in detail. We were able to find clear evidence of the aerosol indirect effects at the Puijo site. There is a positive correlation between cloud droplet number concentration and particle number concentration. Higher cloud droplet concentration led to a smaller average cloud droplet size. Furthermore, the ratio of cloud droplet number concentration to accumulation mode particle number concentration is smaller when the particle number concentration is higher. Results from our trajectory analysis indicated that at our site marine air masses had higher particle concentrations and the continental aerosols are more effective in acting as cloud condensation nuclei than marine aerosols, probably due to their larger mean size. We could also distinguish the effect of local pollutant sources.

Introduction

Anthropogenic aerosol particles such as sulphate and carbonaceous aerosols have substantially increased the global mean burden of aerosol particles from the pre-industrial times to the present-day. Our ability to predict the current and future behaviour of the Earth's climate system is hindered seriously by the large uncertainties associated with the indirect effects by atmospheric aerosols (Lohmann and Feichter 2005). These effects can be estimated from satellite data (Brenguier *et al*. 2003, Sekiguchi *et al*. 2003), by modelling (Menon *et al*. 2002, Rotstayn and Liu 2005) or by measurements (Coakley and Walsh 2002, Wang *et al*. 2008).

The Intergovernmental Panel on Climate Change considers the indirect effects of aerosols to be one of the most uncertain components in forcing of climate change over the industrial period (IPCC 2007). This indirect forcing is caused by the ability of aerosol particles to act as cloud condensation nuclei (CCN) or ice nuclei. With increasing CCN number concentration, caused by human activity, more and smaller droplets are formed. As a consequence, and under the assumption that the mass of the water in a cloud (liquid water content, LWC) stays constant, the cloud albedo and thus the reflection of solar radiation increase (Twomey 1977). In addition, the reduction of cloud droplet size may weaken precipitation development, resulting in more persistent clouds (Albrecht 1989), although the opposite is also possible (Han *et al*. 2002). Many of these climatically important cloud properties depend strongly on atmospheric aerosol particles. Only few measurement stations, e.g. the Global Atmospheric Watch stations at Pallas, Finland (e.g. Komppula *et al*. 2005) and at Jungfraujoch, Switzerland (e.g. Henning *et al*. 2002), have been able to provide valuable long-term data on aerosol–cloud interactions.

A new measurement station for aerosol–cloud interactions has been established on the top of the Puijo observation tower, located in Kuopio, Finland (Leskinen *et al*. 2009). This paper aims to: (1) provide the first characterization of the aerosol–cloud interactions at the Puijo station in a semi-urban environment, (2) quantify some parameters of aerosol indirect effect at the site, and (3) separate these main parameters between different air masses and sources. A very useful feature of our measurements is that they are a part of a continuous monitoring program. This makes it possible to capture a large set of cloud events to analyze statistical dependences between different aerosol populations and various meteorological factors.

Methods

Site description

The Puijo station was established in 2005 by the Finnish Meteorological Institute and the University of Kuopio. The station is located on the top floor of the Puijo observation tower (62°54´32´´N, 27°39´31´´E, 306 m a.s.l., 224 m above the surrounding lake level), which is situated in the town of Kuopio (central Finland, about 330 kilometres to the north from Helsinki), in a semi-urban environment.

The station provides continuous data on particle and cloud droplet size distributions, optical properties of particles, various weather parameters and concentration of some trace gases. In addition, intensive measurement campaigns have been organized yearly in co-operation with the University of Kuopio (October–November 2006, August–September 2007, September–October 2008). During these campaigns, we also measured aerosol chemical composition, particle hygroscopicity, cloud condensation nuclei concentration and collected cloud water samples for chemical analysis. Since we focus on particle and cloud droplet data, we explain only these measurements in more detail in this paper. For a more complete presentation of the station and the instrumentation, *see* Leskinen *et al*. (2009).

Cloud droplet measurements

We used a cloud droplet probe (CDP, Droplet Measurement Technologies) to measure the cloud droplet size distribution in the diameter range of 3–50 μm. The device uses a laser beam with a wavelength of 658 nm to detect the droplets and classify them according to their size. By knowing the sampling area of the laser beam and the sample velocity, we are able to calculate the cloud droplet number concentration in each size class and combine them to get the size distribution. We calculate the average droplet diameter as an average from the number size distribution and the cloud liquid water content from the volume distribution.

The device is mounted on a swivel, which keeps the inlet facing the wind. The laser optics of the CDP are quite weather sensitive, so it has to be switched off during summer and winter in order to protect it from the heat of direct sunlight and low temperatures, respectively. Also in winter, the device gets easily clogged with snow and ice. We estimate the accuracy of the instrument to be around 20%–30% which is typical for other devices based on the same detection principle (e.g. forward scattering spectrometer probe, FSSP).

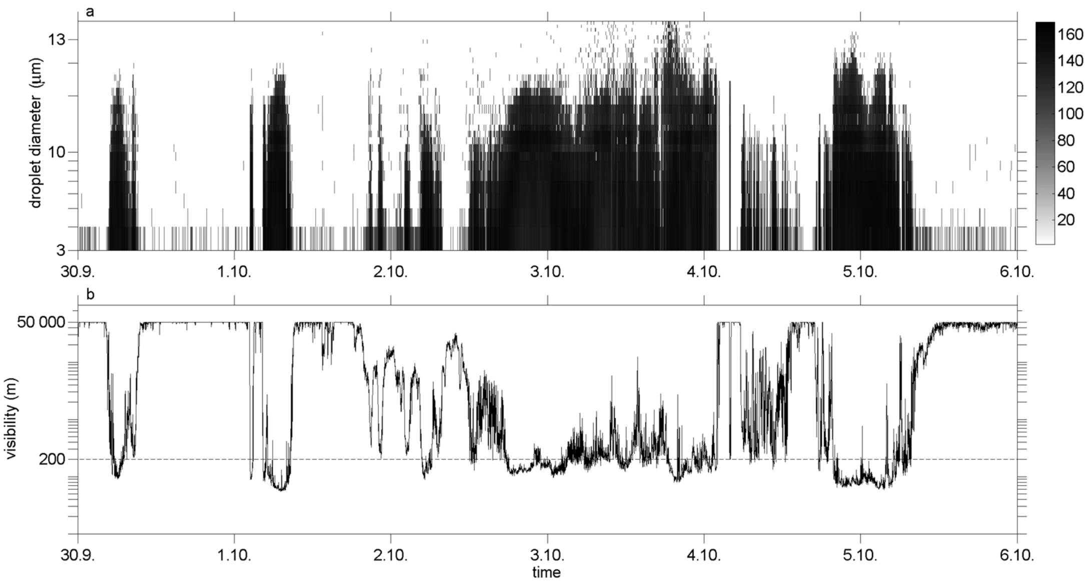

Fig. 1. Example of cloud droplet number size distribution and visibility data. Time period is 30 Sep.–5 Oct. 2008. Four cloud events (30 Sep., 1 Oct., 2 Oct.–4 Oct. and 4 Oct.–5 Oct.) can be seen clearly. The greyscale bar indicates cloud droplet concentration (cm^{-3}).

Particle measurements

The particle number size distribution measurement system at Puijo makes it possible to observe separately the total (out-of-cloud) and interstitial (in-cloud) particle size distributions. It consists of two differential mobility particle sizers and two parallel sampling lines. The sampling line for cloud interstitial aerosol has a PM10 inlet followed by a PM2.5 cyclone. The total air sampling line has a heated hood, with a cut-off size of 40 μm, and is heated in order to dry the cloud droplets. However, the dual inlet system is still under validation and thus we are using data from the total air sampling line only. The aerosol sample is drawn through the sample line through the roof of the tower. The length and inner diameter of the sample line are 6.1 m and 60 mm, respectively, and we correct the data for sampling losses. The measured aerosol size range was 10–500 nm until March 2007 and 7–800 nm thereafter. We also have a condensation particle counter (TSI 3010) in parallel with the DMPS system, in order to measure the total number concentration of particles.

Data evaluation

The particle population is often divided into nucleation mode, Aitken mode and accumulation mode. Here we will use size limits 7–25 nm, 25–100 nm and 100–800 nm for the different modes, respectively. From the cloud activation point of view, Aitken and accumulation mode are mainly involved in cloud formation.

With the measurement system at Puijo, we are able to study the activation of aerosol particles into cloud droplets during cloud events. These events are characterized by a sudden drop in visibility and a burst in cloud droplet concentration (Fig. 1). Since rain drops remove unactivated aerosol particles and would disturb our analysis, we exclude all rainy cloud events. We have also recently installed a weather camera on the top of the tower which allows us to check the prevailing weather conditions. It provides us still images, so cloud occurrence can be confirmed afterwards if needed.

The first step of our data analysis was to calculate hourly averages of the weather parameters and particle and cloud droplet size distribution data. After this, we classified all hourly averages with visibility below 200 m and rain intensity

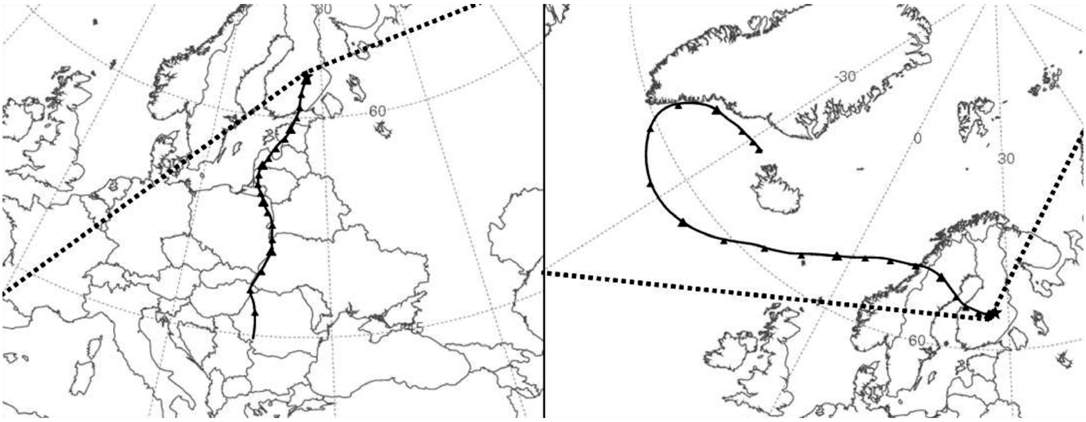

Fig. 2. Examples of typical continental (left) and marine (right) air mass trajectories arriving to the Puijo station. Also shown are the sector limits used to classify air mass origins.

below 0.2 mm h^{-1} as cloud event hours.

We classified the particle concentration data into four groups based on the aerosol particle number concentration in order to better distinguish the correlations between concentration and various parameters involved in cloud–particle interaction. To get groups with equal amount of data, we will used the following concentration limits: < 700 cm^{-3}, 700–1300 cm^{-3}, 1300–2200 cm^{-3} and > 2200 cm^{-3}. We then calculated the average cloud droplet concentration N_d, average droplet diameter d_d, accumulation mode particle concentration N_{acc}, ratio of N_d to N_{acc}, ratio of Aitken mode particle concentration N_{ait} to accumulation mode particle concentration N_{acc} and liquid water content LWC for each concentration range.

We had calculated 120-hour backward trajectories to be able to classify the air masses and to evaluate the differences between marine and continental aerosol. The classification between marine and continental was made visually from the trajectory plots for each event. To avoid any bias in the classification we selected only clearly continental cases as "continental" and likewise for the marine. In our classification, the continental air masses had not spent time over sea during the last 120 hours, whereas the "marine" air masses arrived straight from the Atlantic or the Arctic Ocean (Fig. 2). It should be noted, however, that these air masses spent on average 40 hours over the continent before arriving at our measurement station and thus can not be considered purely marine. The rest of the cases were classified as "mixed". The mixed cases will also be presented in the analysis, but the main emphasis is on the separation of marine and continental air masses.

To inspect the effect of local pollutant sources, we classified the cloud event data in four groups according to the wind direction. The first sector (0° (north) to 45°) encompasses air masses from a pulp mill, located about 5 km to the north-northeast of the tower. The second sector is to the east (45°–157.5°), to the direction of the centre of Kuopio, which is about 2 km southwest of the tower and at about 200 meters lower in altitude. The third sector is straight to the south (157.5°–202.5°), where a heating plant is located roughly 3 km from the tower. The last sector, encompassing an area from 202.5° to 360°, has no important local sources. In addition to the sources listed above, there is also an important highway 1–3 km from the tower in the direction of sectors 1–3.

We also estimated the indirect effect, IE, with the equation

$$\mathrm{IE} = \frac{1}{3}\frac{d\ln N_d}{d\ln\alpha} \tag{1}$$

where N_d is the cloud droplet number concentration and α is some property of the particle population, e.g. aerosol optical depth, light scattering coefficient or particle number concentration (McComiskey and Feingold 2008). We used the readily available total particle number concentration for α, as was done by Lihavainen *et al.* (2008).

Results and discussion

Summary of the cloud events

Between June 2006 and October 2008, roughly 160 cloud events occurred at Puijo. Most of the events took place in the autumn and early winter, November being the cloudiest month with low level clouds occurring on 42% of the time (Fig. 3). The annual average cloudiness percentage at Puijo was 10%. Icing conditions ($T < 0$ °C) were observed throughout the winter. The duration of the cloud events ranged from 15 minutes to 56.5 hours. In the further analysis we use hourly averages as described in the previous chapter, excluding the shortest cloud periods. Due to the lower cut-off size of 3 μm of the CDP, we are not able to detect liquid water content lower than approximately 0.02 g m^{-3} for cloud droplet number concentrations above 400 cm^{-3}. Thus, in the following analysis we will neglect all data with LWC lower than 0.02 g m^{-3} in order to get representative distribution for cloud droplet number concentrations. This way we have 356 hours of data for a more detailed analysis.

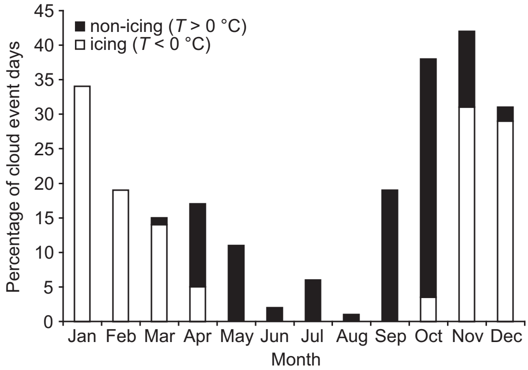

Fig. 3. Average monthly percent of cloud event days for the time period June 2006–October 2008.

Overview of the cloud physical properties

We found that the cloud droplet number concentration was highest in the autumn and lowest in the spring (Fig. 4a). The droplet concentration was 665 cm^{-3} at its maximum and 138 cm^{-3} on average. In these clouds, the average cloud droplet diameter ranged from 3.2 to 16.6 μm with no systematic annual variation in the average cloud droplet size (Fig. 4b). The liquid water content in the clouds had a maximum value of 0.080 g m^{-3}, being 0.039 g m^{-3} on average (Fig. 4c). These values are comparable to other observations in low level clouds given by Miles *et al*. (2000).

Overview of the particle properties

We found that during June 2006–October 2008 the long-time average of the hourly total particle concentration was 2054 cm^{-3}. The particle concentration was highest in the spring and lowest in the autumn (Fig. 5a). We found that the concentration of Aitken (Fig. 5b) and accumulation mode (Fig. 5c) particles followed the same annual pattern. Of special interest to us was the ratio N_{ait}/N_{acc} since accumulation mode particles are more active in cloud droplet activation and the ratio can give some indication of the aerosol sources. The ratio has a median value of 2.35. Since it is hard to see a clear annual trend, (Fig. 5d), we calculated medians of the ratio for winter (December–February), spring (March–May), summer (June–August) and autumn (September–November) and obtained the values 2.38, 2.51, 1.93 and 2.59, respectively. High values during the spring and autumn are explained by nucleation events and cloud events, respectively. During the winter the ratio is also quite high as compared with that in the summer. This may partly be explained by the fact that quite many cloud events took place also in December and January (Fig. 3).

Cloud droplets *vs*. particles — the indirect effects

Effect of particle number concentration

Based on the particle concentration classification given above, we found three clear indications of the aerosol indirect effects at our site (Table 1): (1) The cloud droplet concentration increased with the increasing particle concentration. (2) The cloud droplet concentration was inversely

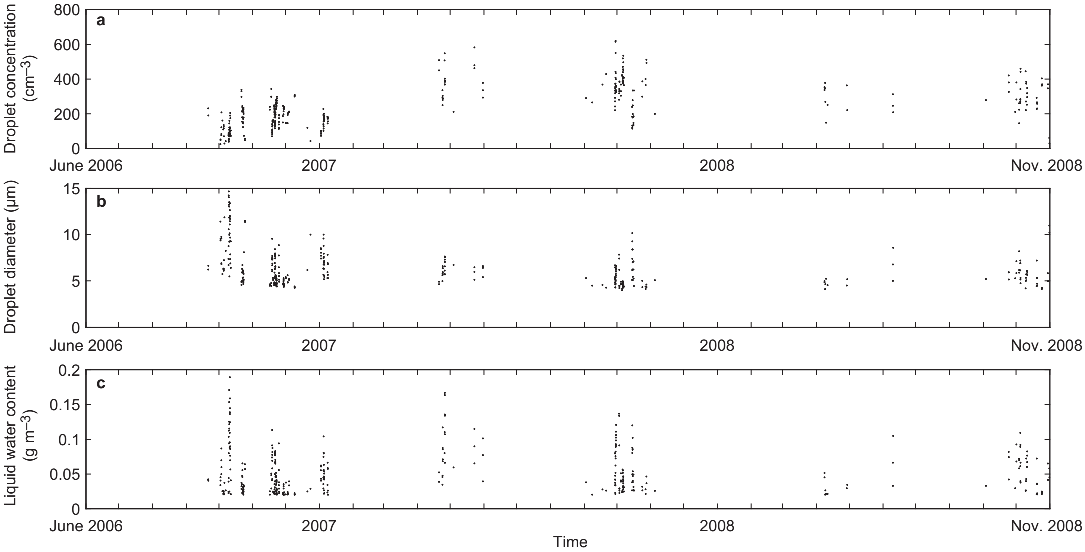

Fig. 4. Time series of cloud droplet data during cloud events. (**a**) Cloud droplet number concentration. (**b**) Average droplet diameter. (**c**) Liquid water content. All values are hourly averages. The cloud droplet probe has been switched off during summers and winters, which causes the gaps in data.

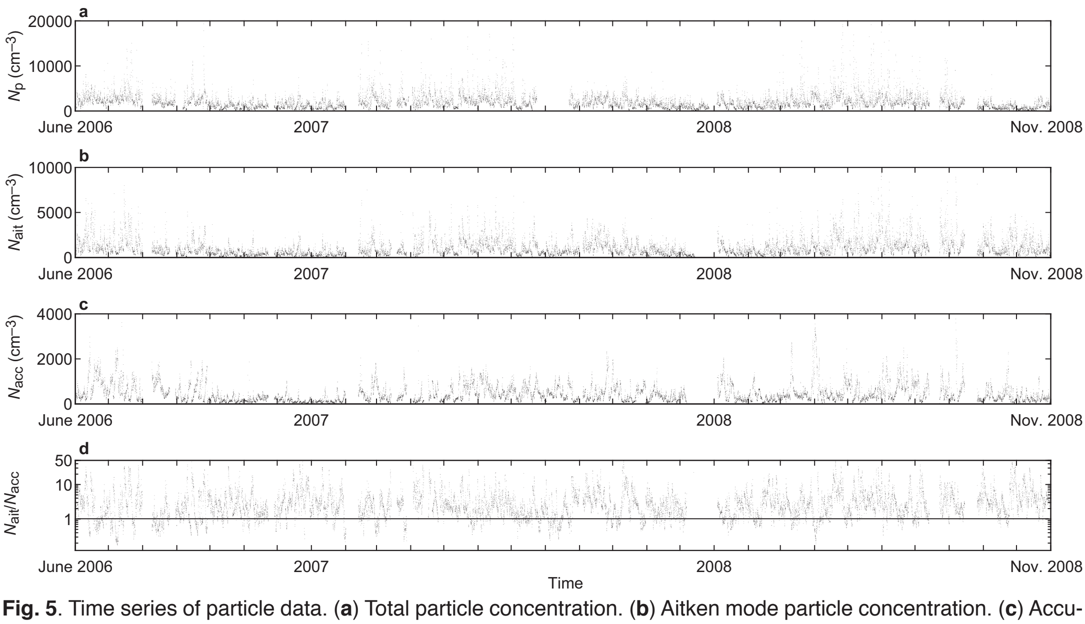

Fig. 5. Time series of particle data. (**a**) Total particle concentration. (**b**) Aitken mode particle concentration. (**c**) Accumulation mode particle concentration. (**d**) N_{ait}/N_{acc}. Total particle concentration is measured with a CPC, others are derived from DMPS data. Note that in **d** *y*-axis is logarithmic.

proportional to the average droplet diameter, as previous studies have shown (e.g. Vong and Covert 1997, Twohy *et al*. 2005, Komppula *et al*. 2005). (3) The ratio N_d/N_{acc} was smaller when particle concentration was higher. There was a slight tendency for the particle concentration to be positivly correlated with the N_{ait}/N_{acc} ratio. The LWC had a maximum value in the first two concentration classes and it seemed to decrease slightly towards larger particle concentrations.

Effect of air mass origin

Marine air masses were characterized by the higher particle number concentration, higher N_{ait}/N_{acc} ratio, smaller droplet number concentration and lower liquid water content as compared with continental air masses (Table 2). The higher N_{ait}/N_{acc} ratio in the marine air masses is consistent with the pronounced Aitken mode of typical marine number size distributions (Anttila *et al.* 2008, Lihavainen *et al.* 2008). The lower particle number concentration in the continental air masses as compared with that in the marine air masses was not what one would expect. It seems that during the cloud events observed here, the continental air masses were relatively clean, the average number concentration being well below the annual average. But overall the continental air masses certainly have their own characteristics, i.e., a different shape of the size distribution.

To evaluate the differences between the air mass classes, we plotted the average hourly droplet concentration as a function of accumulation mode particle concentration for each air mass class and fitted a curve of the form $y = ax^b$ to the data (Fig. 6a and Table 3). We also checked out how the droplet concentration behaves as a function of combined Aitken mode and accumulation mode concentration (Fig. 6b). In our analysis we are able to distinguish the difference between the marine and continental air masses. The continental aerosols are more effective in acting as CCN than marine aerosols (Fig. 6a), probably due to different shapes of the size distributions.

To find out if this difference in activation efficiency is statistically significant, we carried out Student's *t*-test on the N_d/N_{acc} data of marine and continental air masses. Test result (*t*-test: $t = 7.7653$, df = 80.391, $p < 0.0001$) indicated that the marine cases differ significantly from the continental cases. However, since the variables were not normally distributed, Student's *t*-test may have given a biased result. We tested normality with Shapiro-Wilk and Kolmogorov-Smirnov tests, and both of them indicate that the variables were not normally distributed. *P* values resulting from the Shapiro-Wilk test were 0.02724 and < 0.0001 for marine and continental cases, respectively. In addition, equality of variances was tested with Levene's test and it suggested that the variances were not equal. Since the assumptions of the *t*-test were not fulfilled, we verified the result of Student's *t*-test with a nonparametric Wilcoxon Rank Sum test ($W = 7183$, $p < 0.0001$) which also indicated that the difference between marine and continental cases is statistically significant.

Table 1. Average values of cloud droplet concentration N_d, droplet diameter d_d, accumulation mode concentration N_{acc}, N_d/N_{acc} and N_{ait}/N_{acc} ratios, and liquid water content LWC for different total particle concentrations N_p during the observed cloud events. The last line shows the overall average values.

N_p (cm^{-3})	N_d (cm^{-3})	d_d (μm)	N_{acc} (cm^{-3})	N_d/N_{acc}	N_{ait}/N_{acc}	LWC (g m^{-3})
< 700	160	7.77	130	1.23	2.41	0.056
700–1300	248	6.16	326	0.76	1.80	0.056
1300–2200	261	5.95	389	0.67	2.72	0.050
> 2200	294	5.37	502	0.59	3.50	0.043
1375	239	6.33	328	0.72	2.47	0.052

Table 2. Average values of cloud droplet concentration N_d, droplet diameter d_d, total particle concentration N_p, ratio of droplet number concentration to total particle number concentration N_d/N_p, accumulation mode concentration N_{acc}, N_d/N_{acc} and N_{ait}/N_{acc} ratios, and liquid water content LWC calculated according to air mass origin during the observed cloud events.

Class	N_d (cm^{-3})	d_d (μm)	N_p (cm^{-3})	N_d/N_p	N_{acc} (cm^{-3})	N_d/N_{acc}	N_{ait}/N_{acc}	LWC (g m^{-3})
Marine	203	6.82	1313	0.15	191	1.06	4.08	0.051
Continental	231	6.55	1160	0.20	334	0.69	1.90	0.058
Mixed	258	5.87	1653	0.16	380	0.68	2.32	0.046

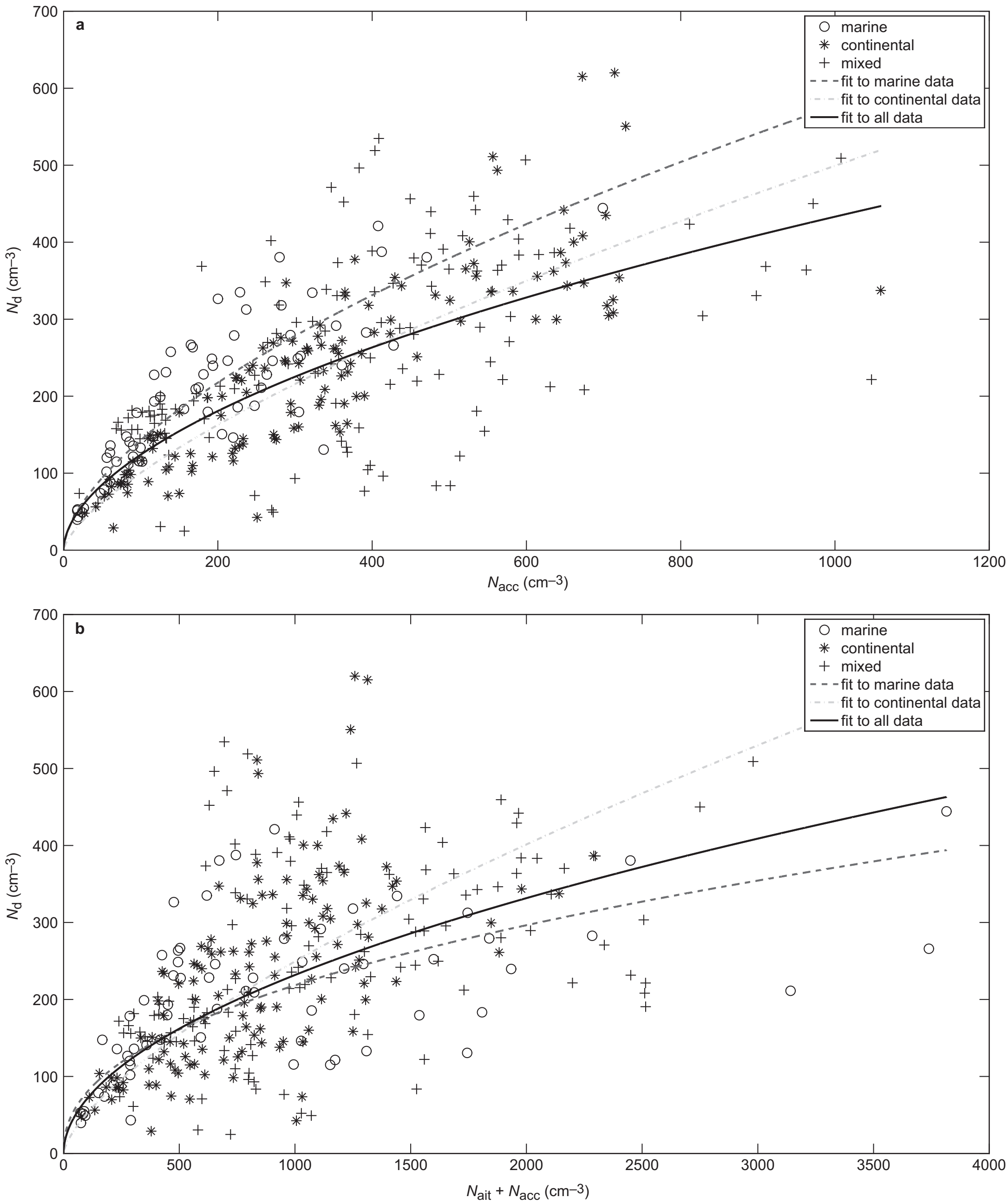

Fig. 6. Droplet number concentration (**a**) as a function of accumulation mode particle concentration, and (**b**) as a function of combined Aitken and accumulation mode particle concentration. Also shown are least-square curves of the form $y = a \times x^b$ (a and b are given in Table 3).

The difference in the activation efficiency may partly be due to the fact that marine aerosols normally have a larger fraction of smaller particles, which are unable to act as CCN. Another explanation is the difference in the particle chemical composition between the air masses. We must also take into account the fact that marine air masses spend on average 40 hours over the continent before arriving at Puijo, which certainly affects the characteristics of the aerosol population.

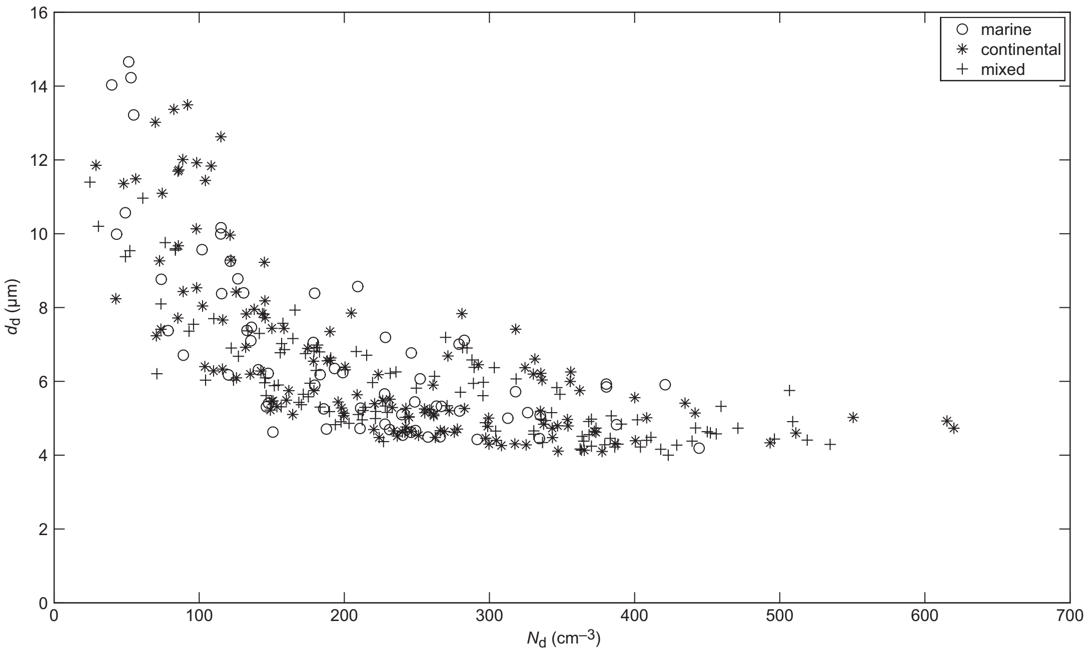

Fig. 7. Average droplet diameter as a function of hourly average droplet number concentration for the time period July 2006–October 2008.

One possible reason for scattering of the data (Fig. 6a and b) are, for example, differences in boundary layer conditions during separate cloud events. Although we tried to screen out all rainy cloud events, it is possible that even a weak drizzle affects our observations. Also, differences in the chemical composition of particles very likely affects the particle activation. These factors, among other variables affecting cloud droplet activation, are discussed in an extensive review by McFiggans *et al*. (2006).

We also plotted droplet diameter as a function of droplet concentration for different air masses (Fig. 7). It is evident that larger droplets are present only when the droplet concentration is lower. Small differences in droplet diameter between different air masses exist only for low droplet concentrations.

For comparison, we plotted our marine and continental observations and exponential fits (Fig. 8a and b, respectively) alongside some similar curve fittings found in literature. When looking at the marine data (Fig. 8a), we note that the curve fittings by Martin *et al*. (1994), Vong and Covert (1998) and Twohy *et al*. (2005) are quite close to our own fit and observations, despite the fact that our marine air masses had spent several days above continent. The small difference is very encouraging and supports our method of distinguishing between marine and continental air masses. However, fits by McFarquhar and Heymsfield (2001) and Lu *et al*. (2007) are considerably different. The reason for this is probably that Lu *et al*. (2007) observed particles larger than 10 nm. McFarquhar and Heymsfield (2001) did not take into account the air mass origin. Their data were obtained over the Indian ocean but the air masses had arrived from elsewhere. In the case of continental data (Fig 8b), it seems that at low particle concentrations our observa-

Table 3. Coefficients for the equation $y = a \times x^b$ used in the least-square fittings and correlation coefficient R for each fit.

Data	a	b	R
N_d *vs.* N_{acc}, marine	8.75	0.61	0.91
N_d *vs.* N_{acc}, continental	4.06	0.70	0.88
N_d *vs.* N_{acc}, all	10.2	0.54	0.75
N_d *vs.* $N_{ait} + N_{acc}$, marine	10.4	0.44	0.73
N_d *vs.* $N_{ait} + N_{acc}$, continental	2.17	0.69	0.71
N_d *vs.* $N_{ait} + N_{acc}$, all	6.52	0.52	0.62

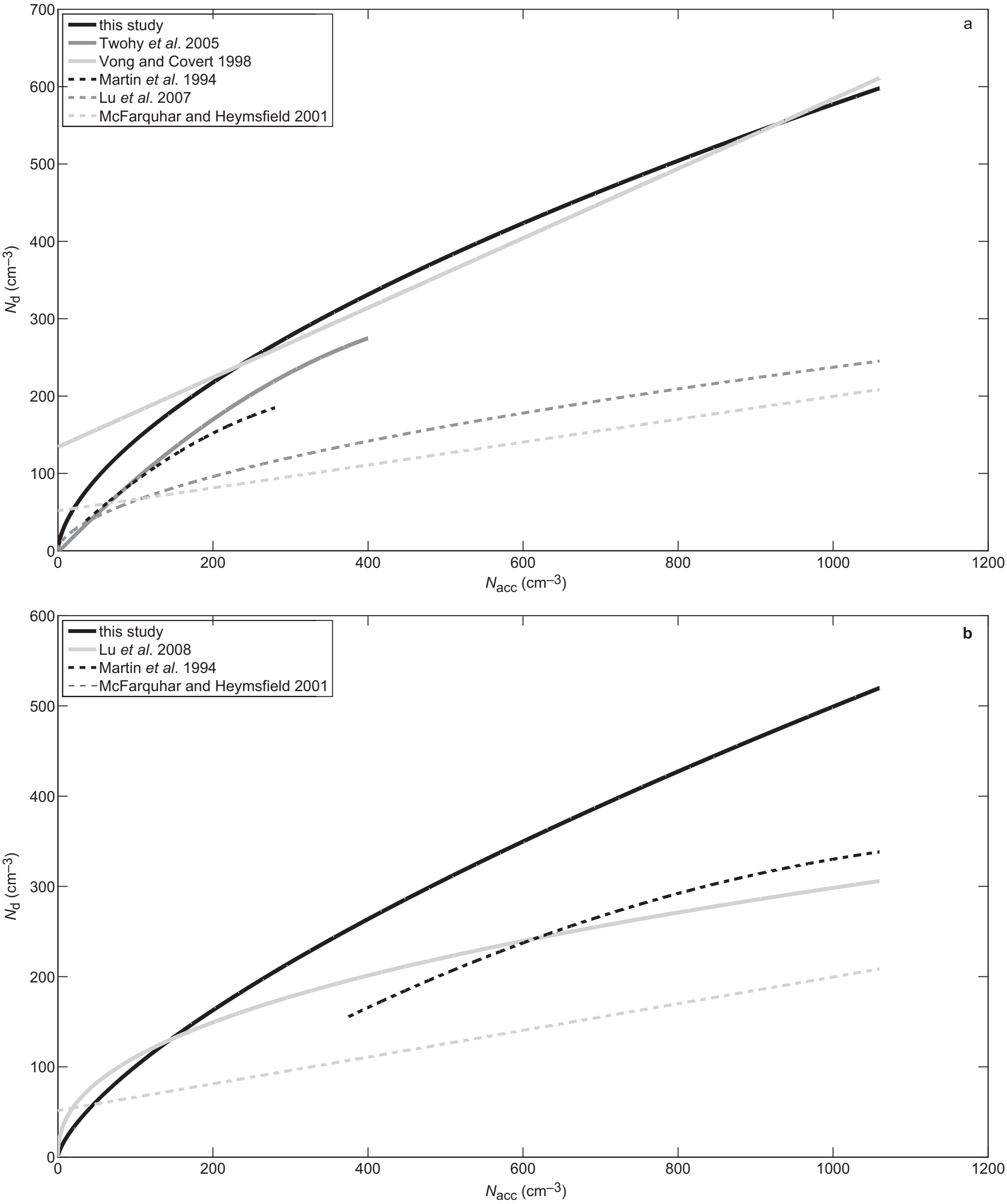

Fig. 8. Droplet number concentration as a function of accumulation mode particle number concentration for (**a**) marine and (**b**) continental air masses. Also shown are least-square curves of the form $y = a \times x^b$ (a and b are given in Table 3) and some similar curve fittings from literature. In **a**, Vong and Covert (1998) used a lower particle size limit of 80 nm and Lu *et al.* (2007) a lower particle size limit of 10 nm. In both **a** and **b**, Martin *et al.* (1994) used a lower particle size limit of 50 nm. The fit by McFarquhar and Heymsfield (2001) is the same in both pictures, since they did not distinguish between air mass sources. They used a lower particle size limit of 20 nm.

tions and the fitting are close to those found in literature (McFarquhar and Heymsfield 2001, Lu *et al.* 2008). At larger particle concentrations, however, the difference is somewhat large. Lu *et al.* (2008) observed clouds at the Gulf of Mexico, and the different environment most probably has some effect on data. Also, Martin *et al.* (1994) observed particles in the diameter range of 0.05 μm–1.5 μm, which may cause the difference. The curve of McFarquhar and Heymsfield (2001) is the same as in the previous picture, with no consideration of air mass origin. As a whole, in both marine and continental air masses, the difference between our data and those found in the literature is larger when the particle size limit is lower. The larger amount of small particles that are unable to act as cloud condensation nuclei lowers the particle activation efficiency.

Effect of local pollutant sources

To find possible differences in particle and cloud droplet data between the wind sectors, we calculated average values of total particle concentration, accumulation mode concentration, ratio of N_d to N_{acc}, N_{ait}/N_{acc}, cloud droplet concentration, droplet diameter and liquid water content LWC (Table 4).

The first sector (0°–45°), including air masses from the pulp mill, is completely different as compared with the other sectors. Surprisingly, the droplet concentration was low and the droplet diameter was more than one third larger than that of other sectors. The particle number concentration was much lower, but the ratio N_{ait}/N_{acc} was high. The high ratio gives an indication of nearby sources, since the ratio tends to decrease with increasing distance from major sources of combustion-derived aerosols. The N_d/N_{acc} ratio was high, but the freshly formed particles in the Aitken mode were probably too small to act as CCN, which kept the droplet concentration low. Also, the liquid water content seemed to be more than twice the value of other sectors. The differences between the other three sectors were not so striking. The third sector (157.5°–202.5°), with the heating plant, had the highest particle concentration.

To justify the data classification according to wind direction as explained in the data evaluation chapter, we analyzed data from our NO_x, ozone and SO_2 measurements (Leskinen *et al.* 2009). The concentration of NO_x and SO_2 was 3–8 times larger for sector 3 (heating plant) as compared with that for the other sectors. Of the other sectors, sector 2 (town and road) shows some tendency to higher NO_x values as compared with sectors 1 and 4 (5%–40%). Sector 1 with the pulp mill has 25%–50% higher SO_2 values than sectors 2 and 4.

Indirect effect

We calculated the indirect effect (IE) with Eq. 1 for marine and continental air masses, obtaining values 0.13 and 0.17, respectively. For all data, IE was 0.14. These values are somewhat lower as compared with those presented in literature. Lihavainen *et al.* (2008) got a value of 0.24 from their measurements at Pallas station. Shao and Liu (2006) presented some IE values from the literature ranging from 0.16 to 0.29. They also calculated IE from data observed over the northeast Pacific near the California coast and obtained a value 0.33. Also McComiskey and Feingold (2008) have done an extensive litera-

Table 4. Average values of cloud droplet concentration N_d, droplet diameter d_d, total particle concentration N_p, ratio of droplet number concentration to total particle number concentration N_d/N_p, accumulation mode concentration N_{acc}, N_d/N_{acc}, N_{ait}/N_{acc}, and liquid water content LWC calculated for four wind direction sectors during the observed cloud events.

Sector	N_d (cm^{-3})	d_d (μm)	N_p (cm^{-3})	N_d/N_p	N_{acc} (cm^{-3})	N_d/N_{acc}	N_{ait}/N_{acc}	LWC (g m^{-3})
0°– 45°	145	9.77	707	0.21	168	0.86	2.77	0.100
45°–157.5°	296	5.75	1283	0.23	420	0.70	1.79	0.050
157.5°–202.5°	237	5.95	1572	0.15	374	0.63	2.19	0.049
202.5°–360°	213	6.48	1407	0.15	251	0.85	3.16	0.049

ture comparison of IE values and gave a range of 0.02–0.33. Bulgin *et al*. (2008) used aerosol optical depth data from satellite measurements to calculate global values for IE and state that IE falls mainly between values 0.1 and 0.16. However, they use a different formula to calculate IE, and Shao and Liu (2006) suggest that values obtained with the equation used by Bulgin *et al*. (2008) are only about a half of those calculated with Eq. 1.

Summary

Particle measurements at Puijo semi-urban aerosol–cloud interaction station have been running continuously since June 2006. During this time, we have detected roughly 160 cloud events. We calculated hourly averages of weather, particle and cloud droplet data for the whole time period June 2006–October 2008. From this data we got 356 hours of cloud event data for further analysis.

We made trajectory analyses to find out the effect of the air mass origin. On average, marine air masses had higher particle concentrations. We were able to distinguish the difference between the marine and continental air masses. It seems that at our site, the continental aerosols are more effective in acting as CCN than marine aerosols. This may partly be due to the fact that marine aerosols normally have larger amount of smaller particles, which are not able to act as CCN. For marine air masses, there were also several cases where droplet diameter was small although the droplet concentration was low.

We found the following clear indications of the aerosol indirect effects at our site: (1) Cloud droplet concentration increased with increasing particle concentration. (2) Increasing cloud droplet concentration lowered the average droplet diameter. (3) Ratio of N_d to N_{acc} was smaller when particle concentration was higher. The effect of air mass origin and local pollutant sources is clearly visible: continental aerosols are very efficient as cloud condensation nuclei, and local polluters affect the aerosol population and this way also the cloud droplet population. We also calculated the numerical value for indirect effect from our data. Our values (0.13 and 0.17 for marine and continental air masses respectively) are comparable to those found in literature (0.02–0.33).

Acknowledgements: Financial support by the Academy of Finland Centre of Excellence program (project nos. 211483, 211484 and 1118615) is gratefully acknowledged. The instrumentation was supported financially by the European Regional Development Fund (ERDF). The authors are very grateful for the technical support of A. Aarva, T. Anttila, A. Halm, H. Kärki, A. Poikonen and K. Ropa from FMI's Observation Services. The authors would also like to thank S. Mikkonen from the University of Kuopio for the help in statistical analysis.

References

Albrecht B.A. 1989. Aerosols, cloud microphysics, and fractional cloudiness. *Science* 245: 1227–1230.

Anttila T., Vaattovaara P., Komppula M., Hyvärinen A.-P., Lihavainen H., Kerminen V.-M. & Laaksonen A. 2008. Size-dependent activation of aerosols into cloud droplets at a subarctic background site during the second Pallas Cloud Experiment (2nd PaCE): method development and data evaluation. *Atmos. Chem. Phys. Discuss.* 8: 14519–14556.

Brenguier J.-L., Pawlowska H. & Schuller L. 2003. Cloud microphysical and radiative properties for parameterization and satellite monitoring of the indirect effect of aerosols on climate. *J. Geophys. Res.* 108(D15), 8632, doi:10.1029/2002JD002682.

Bulgin C.E., Palmer P.I., Thomas G.E., Arnold C.P.G., Campmany E., Carboni E., Grainger R.G., Poulsen C., Siddans R. & Lawrence B.N. 2008. Regional and seasonal variations of the Twomey indirect effect as observed by the ATSR-2 satellite instrument. *Geophys. Res. Lett.* 35, L02811, doi: 10.1029/2007GL031394.

Coakley J.A. & Walsh C.D. 2002. Limits to the aerosol indirect effect derived from observations of ship tracks. *J. Atmos. Sci.* 59: 668–680.

Han Q., Rossow W.B., Zeng J. & Welch R. 2002. Three different behaviors of liquid water path of water clouds in aerosol-cloud interactions. *J. Atmos. Sci.* 59: 726–735.

Henning S., Weingartner E., Schmidt S., Wendisch M., Gäggeler H.W. & Baltensberger U. 2002. Size-dependent aerosol activation at the high-alpine site Jungfraujoch (3580 m a.s.l.). *Tellus* 54B: 82–95.

IPCC 2007. *Climate change 2007: The physical science basis*. Intergovernmental panel on Climate Change, Cambridge University Press, New York.

Komppula M., Lihavainen H., Kerminen V.-M., Kulmala M. & Viisanen Y. 2005. Measurements of cloud droplet activation of aerosol particles at a clean subarctic background site. *J. Geophys. Res.* 110, D06204, doi: 10.1029/2004JD005200.

Leskinen A., Portin H., Komppula M., Miettinen P., Arola A., Lihavainen H., Hatakka J., Laaksonen A. & Lehtinen K. E. J. 2009. Overview of the research activities and results at Puijo semi-urban measurement station. *Boreal Env. Res.* 14: 576–590.

Lihavainen H., Kerminen V.-M., Komppula M., Hyvärinen A.-P., Laakia J., Saarikoski S., Makkonen U., Kivekäs N., Hillamo R., Kulmala M. & Viisanen Y. 2008. Measurements of the relation between aerosol properties and microphysics and chemistry of low clouds in northern Finland. *Atmos. Chem. Phys.* 8: 6925–6938.

Lohmann U. & Feichter J. 2005. Global indirect aerosol effects: a review. *Atmos. Chem. Phys.* 5: 715–737.

Lu M.-L., Feingold G., Jonsson H.H., Chuang P.Y., Gates H., Flagan R.C. & Seinfeld J.H. 2008. Aerosol-cloud relationships in continental shallow cumulus. *J. Geophys. Res.* 113, D15201, doi:10.1029/2007JD009354.

McComiskey A. & Feingold G. 2008. Quantifying error in the radiative forcing of the first aerosol indirect effect. *Geophys. Res. Lett.* 35, L02810, doi: 10.1029/2007GL032667.

McFiggans G., Artaxo P., Baltensperger U., Coe H., Facchini M.C., Feingold G., Fuzzi S., Gysel M., Laaksonen A., Lohmann U., Mentel T.F., Murphy D.M., O'Dowd C.D., Snider J.R. & Weingartner E. 2006. The effect of physical and chemical aerosol properties on warm cloud droplet activation. *Atmos. Chem. Phys.* 6: 2593–2649.

Menon S., Del Genio A.D., Koch D. & Tseloudis G. 2002. GCM simulations of the aerosol indirect effect: Sensitivity to cloud parameterization and aerosol burden. *J. Atmos. Sci.* 59: 692–713.

Miles N.L., Verlinde J. & Clothiaux E.E. 2005. Cloud droplet size distributions in low-level stratiform clouds. *J. Atmos. Sci.* 57: 295–311.

Rotstayn L.D. & Liu Y. 2005. A smaller global estimate of the second indirect aerosol effect. *Geophys. Res. Lett.* 32, L05708, doi:10.1029/2004GL021922.

Sekiguchi M., Nakajima T., Suzuki K., Kawamoto K., Higurashi A., Rosenfeld D., Sano I. & Mukai S. 2003. A study of the direct and indirect effects of aerosols using global satellite data sets of aerosol and cloud parameters. *J. Geophys. Res.* 108(D22), 4699, doi:10.1029/2002JD003359.

Shao H. & Liu G. 2006. Influence of mixing on evaluation of the aerosol first indirect. *Geophys. Res. Lett.* 33, L14809, doi: 10.1029/2006GL026021.

Twomey S. 1977. The influence of pollution on the shortwave albedo of clouds. *J. Atmos. Sci.* 34: 1149–1152.

Twohy C.H., Petters M.D., Snider J.R., Stevens B., Tahnk W., Wetzel M., Russell L. & Burnet F. 2005. Evaluation of the aerosol indirect effect in marine stratocumulus clouds: droplet number, size, liquid water path, and radiative impact. *J. Geophys. Res.* 110, D08203, doi:10.1029/2004JD005116.

Vong R.J. & Covert D.S. 1998. Simultaneous observations of aerosol and cloud droplet size spectra in marine stratocumulus. *J. Atmos. Sci.* 55: 2180–2190.

Wang J., Lee Y.-N., Daum P.H., Jayne J. & Alexander M.L. 2008. Effects of aerosol organics on cloud condensation nucleus (CCN) concentration and first indirect aerosol effect. *Atmos. Chem. Phys.* 8: 6325–6339